

# Quantum Population Dynamics: A Broad View from an Exploration beyond the Standard Model

Jean-Pierre Blanchet\*

ISE, Université du Québec Montréal, 201 Ave du Président Kennedy, Montréal, QC, H3C 3P8, Canada

Received: 2 Apr. 2015, Revised: 19 Jul. 2015, Accepted: 21 Jul. 2015

Published online: 1 Aug. 2015

**Abstract:** To explore quantum and classical connection from a new perspective, a Quantum Population Dynamics (QPoD) model based on the logistic relation common to several sciences is investigated from a very broad perspective to explore the numerous links to current physics. From postulates of causality and finiteness a classical quantum entity, a quanta of spacetime, is defined with unitary extension and intensity. Applying the logistic equation to a quantum population of non-local two-state oscillators results in a quantum-classical equation linking wave and particle dynamics with an explicit account of decoherence. Varying over 124 orders of magnitude, the coupling constant acts like a delta Dirac function between regimes. The quantum regime is conform to Schrödinger and Dirac equations according to respective Hamiltonian while the classical mode suppresses the quantum wave function and follows the Hamilton-Jacobi equation. Besides the quantum wave solutions, in the classical range, the general equation admits Fermi-Dirac and Bose-Einstein solutions, relating to thermodynamics. Inertial mass is found in terms of the quantum entropy gradient. The most compact quantum cluster forming a crystal produces a unique flat space filling lattice cells of one simple tetrahedron and one composite truncated tetrahedron corresponding respectively to a fermionic cell and a bosonic cell. From this lattice geometry alone, the mass ratios of all fermions are expressed uniquely in terms of vertices and faces, matching charges properties of three generations and three families. Except for a minor degeneracy correction, the solution is shown to follow the logistic dynamics. The resulting mass equation is a function of dimensionless natural numbers. Many properties of the Standard Model are recovered from geometry at the Planck scale, respecting naturalness, uniqueness and minimality. QPoD may help addressing questions about the nature of spacetime and the physical microstructure of particles. The model predicts a single spinless matter particle of a 4th generation as a WIMP particle close to Higgs mass.

**Keywords:** Nonlinear dynamics, chaos, foundation of quantum mechanics, modeling, beyond Standard Model, philosophy of science.

## 1 Introduction

The interpretation of quantum mechanics (QM) remains until this day undetermined. It has been argued that this ambiguity is a limiting factor to pursue fundamental research in the domain. Many avenues have been proposed to address the issue. The problem could be traced back to lacking demonstration based on a physical model of spacetime at the finest scale. Indeed, the most fundamental equations of QM were posed heuristically, well supported by experimentation, but not derived explicitly from a first principle basis. Admittedly, the current approach is one attempt to explore the issue from a model of spacetime at the Planck scale. As indicated by the title, it is an exploration effort from an unconventional perspective inherited from complex systems observed in our environment. The depth is still exploratory along a

research path deliberately kept as simple as possible. The scope is purposely broaden to link with established physics. Rather than pretending to an advanced solution, we suggest simply that a population model inspired by environmental sciences may have some implications in theoretical development along a natural line of investigation.

The motivation of this article is to explore the foundation of QM from a new perspective, applying a logistic model commonly used in biology, economics, condensed matter and environmental sciences [1, 2]. The logistic equation describes a situation where the population growth rate of some object density is constrained by available resources following a quadratic relation that is an exponential growth bounded by remaining available resource or accommodation space. May [3] has demonstrated the richness of logistic

\* Corresponding author e-mail: [blanchet.jean-pierre@uqam.ca](mailto:blanchet.jean-pierre@uqam.ca)

solutions, ranging from stable fixed points, to harmonic oscillations, all the way to complex chaotic organization and nearly random solutions. Along the way, it produces rich streams of intermittency and orderly chaos in a huge range of behaviors found in nature. In classical physics, this wide range of behaviors has been illustrated by Couder et al [4] for dynamics of bouncing droplets with regimes ranging from simple bouncing, to period doubling, to chaos and all the way to Faraday stochastic instability. In their experiment, Brady and Anderson [5] demonstrated that a “walkers” range is established where the classical droplets wave coupling reproduced many of the known quantum physics behaviors previously unexpected in classical physics. The bifurcation and period doubling diagram [6] of the bouncing droplets is similar to that obtained from the logistic equation.

However, in application to complex environmental systems like in population ecology, the logistic equation is at best a fair approximation and certainly not an exact solution. It represents well the evolution of a population where the parents are removed from the following generation that is, each generation is made of a new population excluding the generators. One can ask to what extent this model approaches an exact solution in the simplest systems. Intuitively, we may expect the ultimate limit of simplicity at the most fundamental level of the quantum world. *A priori*, it can be a realm where no variable and no constant exist apart from a unitary entity responding only in terms of natural count numbers of occurrence or not. To represent potentially our universe, such a simple world must have unique solutions leading to experimentally observed properties in elementary particles, like symmetries, mass relation and generations of fermion or coupling constants. Hopefully, it might predict new particles or propose testable experiments.

In this paper, our approach is to explore the logistic behavior of a simple quantum entity. Currently, physics is left with more than two dozens of unsolved problems pointing to a common solution at the Planck scale. Two leading issues singled out at the Loop-13 conference<sup>1</sup> on quantum gravity (QG) are the composition of spacetime and the micro structure of elementary particle. The current work examines a possible solution from a systemic point of view.

Considerable progress has been made within the area of QG, in particular, in causal numerical methods at the Planck scale. Stochastic causal set approaches [7-10] to quantum gravity are being developed. Spacetime is discretized by point events and distributed to remain invariant under Lorentz transformation. The number of points determines the volume of spacetime. A partially ordered (poset) and locally finite causal set (causet) respects causality and may be simulated by stochastically sprinkling points of causets following a Poisson’s law of

rare events. In principle, a random causet can be modulated by QM rules for a discrete solution.

Another innovation is in the area of Causal Dynamical Triangulation (CDT) [11-13] where an N-simplex discretization of space respecting causality along the time axis, dynamically converges to 4D spacetime consistent with observations. More recently, has emerged the tensor model [14] exploration in combinatorial mathematics applied to QG and integrating colored triangulations in a general framework. Many approaches to QG use triangulation and N-simplex to discretize spacetime. Together, causet and CDT provide numerical methods to visualize physics at the Planck scale. In this work, a classic population dynamics of a two-state quantum oscillator with a triangular discretization is used to explore some properties of spacetime and elementary particles. In particular, we are interested in the wave-particle duality at the quantum-classic boundary and the implied topology of oscillation modes at the Planck scale from the logistics relationship.

The paper starts by introducing the general concept of the proposed model with a broad view of its potential links to the standard physics. Next, the model development is formulated. It is shown to be consistent with Schrödinger and Dirac equations in the quantum limit while approaching the Hamilton-Jacobi equation in the classical limit. The solution of the model are concomitant to statistical mechanics and thermodynamics. Next, the compact geometry of quantum entities is compared to the elementary particles of the Standard Model. A direct comparison of experimentally observed fermion masses ratio as a function of geometry (vertices and faces occupancy) is made against the solutions from the model. Then, an empirical fit of the known mass ratios is done to demonstrate the naturalness of the elementary particle masses and their structure in 3 generations. Finally, some implications are discussed and summarized in conclusions.

## 2 Model Concept and Rational

Before exploring this question, let us describe the conceptual framework of our exploration “model” in a qualitative way. In this section, defining the model concept is not derived from principles, but it represents one’s working hypothesis and a prerogative of the modeler to explain his viewpoint. We assume a universe made of a finite, but large number of a simple basic entity. The simplest entity is a maximally symmetric 4-sphere with a unitary “extension” diameter of one Planck length and a unitary “intensity” of one quantum of action ( $\hbar$ ). On a scale much larger than the Planck scale, a large population of quanta forms a discrete physical manifold of spacetime with variable density that we interpret as curvature in the scalar field. One can view this very thin

<sup>1</sup> Loop-13 Conference: Conclusion by Carlo Rovelli, Perimeter Institute, Waterloo, July 22-26, 2013. <http://pirsa.org/displayFlash.php?id=13070083> at 31:45 min.

4D quantum substance as a kind of aether<sup>2</sup> made of static finite 4D volume entities with Planck size or as finite points in a Minkowski flat space. Projecting a quantum cluster in 3D can be regarded as an instantaneous spacelike density with a particular configuration state of the quantum subpopulation. A quantum state of that population distribution varies discretely in both time directions (positive or negative) as a succession of 3D state configurations in each Planck time slice  $\delta t = t_p$ . Time is a bi-directional succession of static instantaneous states occurring at once in the causal manifold, i.e. a set of quanta present in a 4D manifold forming a spacetime “patch.” For the energy of one quantum to remain positive, a negative action unit ( $-h$ ) must correspond to a negative time direction

$$E_p = \pm h / \pm t_p = 7.671 \times 10^{19} \text{ GeV} = 1 \text{ n.u.}$$

This is a large value, but with extremely rare occurrence at the Planck scale under normal laboratory conditions.

Planck’s law may be written in term of a single integer ratio within a discrete time frame ( $\delta t = t_p$ ) by changing variable  $\nu = 1/Jt_p$

$$E = nh\nu = nh/Jt_p = P'h/t_p = P'E_p$$

where  $P' = n/J$ ,  $n$  and  $J$  are integer numbers and  $P'$  is a rational number that can be interpreted as a normalized population density between 0 and 1, i.e. from a perfect vacuum to the Planck density limit. It is the probability that one Planck volume be occupied by one quantum of  $h$ .

Conversely, the equivalent total population number of any object can be define as

$$P = \frac{mc^2}{E_p} \tag{1}$$

where  $m$  is the mass of the object and  $c$  the speed of light constant. The space mean quantum population density  $\mathcal{P} = P/\mathcal{V}$  as illustrated in Table 1, is taken over a characteristic volume  $\mathcal{V}$  of the regions per time scale unit.

In our model, a quantum entity is motionless by definition as it exists for only one Planck time, in one Planck unit of the spacetime volume. Each time slice of one Planck thickness represents a new population state, i.e. a reorganization of the constant total number of quanta in the whole universe. A discrete configuration of quanta, a quantum state fabric, is interpreted as our usual physical space, which is a smooth manifold on the large scale. The variation of that quantum space state is the corresponding physical time, an observable in classical physics. In other words, spacetime is a physical substance made of high-energy quanta with large local variation in

population density. The Laplacian of the quantum population density defines spacetime curvature. All observables, variables, micro or macroscopic objects are structured states or normal modes of a quantum population. Far away from the Planck scale, the population density converges to a continuous function.

Dynamical behaviors appear as a simple generation rule of fixed instantaneous quantum population density. Each quantum occurrence is a particular solution of a dynamics equation, and the quantum manifold includes at once all possible solutions of outcomes of a probable interaction. The dynamical rule is that the quantum generation rate in any region is proportional to the population density of the previous generation alone in that neighborhood, i.e. by analogy to living populations in biology where the total number of siblings is proportional to the number of parents in the same region of arbitrary size. Quantum regeneration is modeled as a stochastic Markovian process only function of the instantaneous local quantum population, which is the action or the Lagrangian density. The solution spreads in both time directions at once. The process is causal, but stochastic. The quantum population can be treated as a causal set. Interaction between two distinct quantum sets (manifolds or particles) is more likely in high population densities of each sets, hence the principle of least action imposing the most probable path in a succession of interactions, mapping our classical observed universe as a small subset of the quantum population where interactions occurs.

Besides finiteness and a generation rule, we must constrain quanta or any physical object composed of quanta to a “non-overlapping” rule. In a physical world, any two (or more) overlapping objects could not be distinct from one another, i.e. could not exist as physically identifiable objects. This non-ambiguity condition rules out the conflicting possibility of quantum collocation. This statement has deep logical consequences as it clearly confines “physical reality” into the much wider mathematical realm where, in principle, two points could be moved to a same location. This non-overlapping rule is the basis for the logistic equation behavior in this model by imposing saturation of the space volume occupancy as a physical limit. At high densities, any compacted quantum population approaches a finite saturation limit. In ecology, this is the equivalent to an asymptotic sustainable living population under constraint of limited resources, here spacetime volume is the resource.

Bringing all quanta from any broad region, say the whole universe to its initial quantum state<sup>3</sup>, the compacted limit forms a finite and unique quantum crystal structure. One cosmological implication is that there is no black hole singularities in the model. It turns out that this single possible lattice structure in its 3D projection bares uniquely the imprint of all known particles. Any spacetime region, containing matter or not,

<sup>2</sup> This quantum aether is regenerated at the Plank frequency, consequently in a Michelson-Morley experiment the speed of light must remain isotropic in conformity with observation.

<sup>3</sup> A finite dimension about the size of a proton  $\approx 10^{-16}$  m with current estimated mass of the visible universe.

**Table 1** Scale analysis (to the order of magnitude) of the estimated mean "local quantum" population density as a function of energy and typical volumes ( $\mathcal{V}$ ). The mean quantum population density per time unit  $\mathcal{P}/t$  is estimated for three scales: laboratory scale  $1m^{-3}.s^{-1}$ , laboratory scale per Planck time step ( $t_p$ ) and at Planck scale (number of action unit per Planck volume). The model assumes global adiabatic expansion of the quantum population from an initial Planck scale to the present-day visible universe.

Objects – Scales	Volume $\mathcal{V}$	Mean Quantum Population Density $\mathcal{P}/t$		
	[m <sup>3</sup> ]	[1/(m <sup>3</sup> s)]	[1/(m <sup>3</sup> t <sub>p</sub> )]	[1/(ℓ <sub>p</sub> <sup>3</sup> t <sub>p</sub> )]
Vacuum <sup>0</sup>	---	10 <sup>24</sup>	10 <sup>-19</sup>	10 <sup>-124</sup>
Mean universe	10 <sup>80</sup>	10 <sup>26</sup>	10 <sup>-17</sup>	10 <sup>-122</sup>
Galaxy <sup>1</sup>	10 <sup>61</sup>	10 <sup>31</sup>	10 <sup>-12</sup>	10 <sup>-117</sup>
Solar System <sup>1</sup>	10 <sup>39</sup>	10 <sup>46</sup>	10 <sup>3</sup>	10 <sup>-101</sup>
Earth	10 <sup>21</sup>	10 <sup>50</sup>	10 <sup>5</sup>	10 <sup>-97</sup>
Hydrogen atom	10 <sup>-30</sup>	10 <sup>50</sup>	10 <sup>5</sup>	10 <sup>-97</sup>
Sun	10 <sup>28</sup>	10 <sup>52</sup>	10 <sup>7</sup>	10 <sup>-95</sup>
<b>Proton</b>	<b>10<sup>-45</sup></b>	<b>10<sup>68</sup></b>	<b>10<sup>23</sup></b>	<b>10<sup>-79</sup></b>
<b>Black hole<sup>2</sup></b>	<b>10<sup>12</sup></b>	<b>10<sup>68</sup></b>	<b>10<sup>23</sup></b>	<b>10<sup>-79</sup></b>
GUT <sup>3</sup>	---	10 <sup>82</sup>	10 <sup>37</sup>	10 <sup>-65</sup>
Electron <sup>4</sup>	10 <sup>-105</sup>	10 <sup>125</sup>	10 <sup>82</sup>	10 <sup>-23</sup>
Top Quark <sup>4</sup>	10 <sup>-105</sup>	10 <sup>131</sup>	10 <sup>87</sup>	10 <sup>-17</sup>
Planck limit	10 <sup>-105</sup>	10 <sup>147</sup>	10 <sup>102</sup>	1

<sup>0</sup> Assuming a vacuum energy density of  $10^{-29}$  gm.cm<sup>-3</sup>

<sup>1</sup> Cylindrical volume estimated as a disk

<sup>2</sup> Spherical volume at the Schwarzschild radius

<sup>3</sup> GUT energy or  $10^{14}$  GeV at the proton scale volume

<sup>4</sup> Planck elementary volume

pressed toward its compact limit will form a black hole. Based on statistical mechanics, the compact crystal lattice is unstable due to an excessive chemical potential over the internal energy of the system<sup>4</sup>. When expanding the compact quantum population volume up to the black hole horizon, the quantum separation increases and the system becomes diluted in analogy to a crystal melting to a liquid phase. Within the black hole horizon, the quantum population is causal. In accord with special relativity (SR), observable time is stretched to a halt. Time is bi-directional, spreading over the entire spacetime region of the black hole history, from creation to dissipation. Individual elementary particles act similarly to BH (Table 1).

Outside the black hole horizon, dilution of the quantum population increases with distance, producing observable curvature of spacetime and phenomena like

<sup>4</sup> This is analogous to bringing all air molecules of a room into one corner, as a classroom illustration.

the gravitational lensing effect. This quantum phase is comparable to a gas where refraction of light is due to molecular density gradients, producing a curvature in the gas density field. With increasing separation, the quantum population density decreases enormously (Table 1) and the global causality is broken up into causal subsets or independent "patches" of quantum populations. This symmetry-breaking condition leads to a second quantization of spacetime. To remain causal, the newly formed pockets of quantum populations (particle manifolds) are specific resonance modes corresponding to elementary particles (e.g. leptogenesis) with definite total action or fixed energy levels according to their mass. The possible solutions are the normal modes of discrete quantum wave solutions that must be allowed as well on the most compact lattice structure found in the saturation limit case. This is a central hypothesis of the model we are investigating, by limiting ourselves to the compact lattice as a particular case, but assuming equivalent



extensions to dispersed quantum distributions. e.g. from translation symmetries. In other words, the resonance mode solutions are a global property of the each particle manifolds, each spacetime "patch".

On the large scale, the process of second quantization of spacetime resulting in causal set of quanta for each particle can be approximated by continuous wave-functions solution of a dynamic equation, as illustrated from second column in Table 1 for a laboratory scale. In principle, the causal region of every particle is unbounded, but in many cases the quantum population density confines more or less each particle to a finite region of spacetime. For instance, an electron in the quantum cloud of an S orbital of the hydrogen atom is strongly constrained by contrast to a photon spacetime stretching in free space from emission source to absorption sink. To various degrees, a particle is non local in spacetime. The degree of particle tunneling effect is directly linked to the degree of spacetime confinement of its quantum population.

On a scale much larger than the Planck scale (say  $10^{-26}$  to  $10^{+26}$  meters), each particle occupies a 4D manifold. A particle manifold has a single entry and one exit locations, corresponding to sites in Minkowski spacetime of creation and annihilation of the particle. At very high quantum dilution found in the mean state of the current universe, manifolds of particles are nearly independent of one another<sup>5</sup>. In the absence of interactions, elementary particles entangled in isolated spacetime pockets are closed systems with bidirectional causal timelines as within a BH horizon. Because of very low quantum densities, these "patches" can overlap and coexist in the same region maintaining their individual coherence. This property is effectively used in quantum computing systems. On very rare occasion two particle manifolds are conflicting when two of their individual quanta attempt to occupy the same location, say a photon interacting with an electron, then the addition of the action<sup>6</sup> pairs ( $+h - h$ ) annihilate each other, collapsing both wave functions and merging the two manifolds into, say a faster electron, for example. The newly combined wave function spreads out again, and perhaps it could break up into a pair production, for example, resetting or collapsing the wave function again, and so on.

Two types of lattice sites occupation are considered, (1) the independent quantum occurrence (most of the cases) and (2) the rare quantum interaction points between two manifolds, as just described. The first type is what we call the quantum world. The second case is the corresponding classical world. The observed precise location is the exact interaction point where, say the photon population cloud has encountered the electron population in our example. The combination of all these

<sup>5</sup> The analogy that I have in mind is the collision of two galaxies where stars do not collide due to distances.

<sup>6</sup> In the model, quantum of action are assumed to have two possible states  $\pm h$  as binary oscillators.

interaction points is our observable universe where the elementary particles appear as point objects and the wave function behavior has collapsed leaving traces of the wave history in interference patterns of a Young's experiment, for instance. All the other independent points (where no interaction is occurring) obey the Schrödinger wave equation for individual particles, leading to the observed non local quantum behaviors and particles entanglement.

In this model, a Dirac quantum field is the superposition of all manifolds subspace of one type of particle, say an electron field made by adding the superposition from all individual electron manifolds over the entire universe. It is the larger quantum population of spin objects (defined in section 4) where particles are indiscriminate, forming a field.

Now that we have set the broad picture, in the following, we will investigate how the standard logistic equation can link quantum and classical physics into a unified description of a quantum population. We hope that some of the prescribed parameters in the standard model could be understood and evaluated on a physical basis from a fundamental framework along the line of the conceptual model.

### 3 Model

To define a self-replicating entity of a quantum population dynamics (QPoD) model, we pose two postulates, causality and finiteness. Causality imposes a causal relation in the time direction, while finiteness assumes that everything in the universe is finite. Finiteness restrains physical objects in the wider mathematical realm by excluding divergent, singular and infinite solutions, but converging to continuous differentiable functions at large scales. Finiteness also accounts for the "non-overlapping" constraint, otherwise an infinite number of entities would be possible in a finite space.

To define a fundamental entity, we consider a two-state quantum of action with a unitary intensity  $h$  and a unitary extension diameter of one Planck unit ( $\ell_P, t_P$ ) in 4D. No other parameters are assumed for this model. Natural constants are implicitly defined by the quantum entity ( $c = \ell_P/t_P = 1$  and  $G = \ell_P^5/\hbar t_P^3 = 1$  in natural units). In 3D, a quantum is like micro black holes (BH) smaller than a Schwarzschild radius  $R_{SP} = 2\ell_P = 2$  and with a reduced Compton wavelength  $\lambda_{CP} = \ell_P = 1$ . From the finiteness postulate, quantum population density  $\mathcal{P} = \mathcal{P}_{sat}$  saturates approaching the singularity in the black hole limit.

In a flat space, the maximally compact quantum population state at saturation  $\mathcal{P}_{sat}$  defines a unique lattice geometry where each cell forms the Brillouin zone of a quantum crystal, as illustrated in Figure 1 for 3D projection. A compact block tessellating 3D space (the blue shape in Figure 1b) is composed of a combination of a tetrahedron (the smallest volume unit) and a truncated tetrahedron (the complementary composite ensemble with

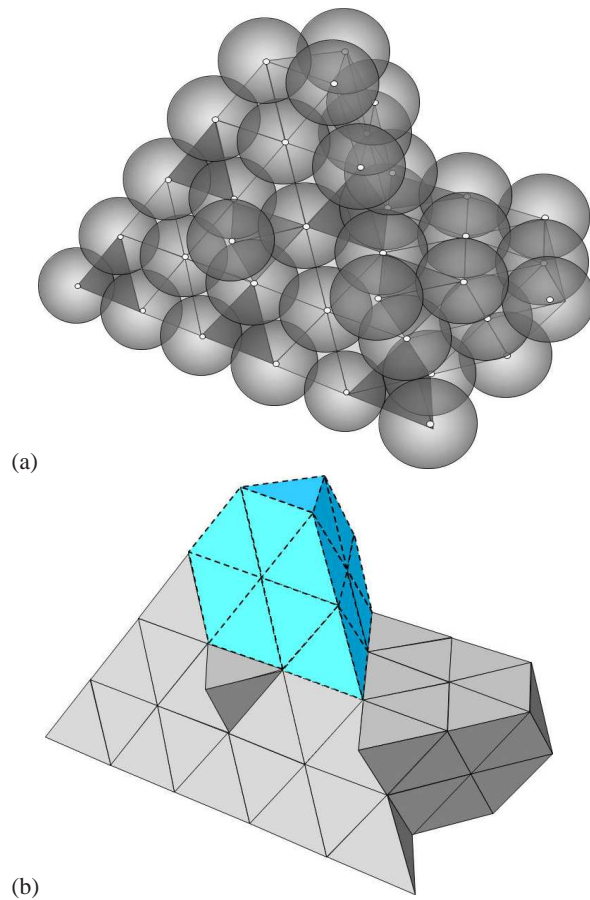


**Fig. 1** 3D illustration of quantum entities (a) in a most compact space filling structure and (b) the corresponding lattice. The blue colored volume is a basic unit tessellating flat space uniformly.

dashed lines in Figure 1b). The small tetrahedron volume is the basic unitary element of the lattice. This Platonic solid has the properties of being the smallest volume with the largest surface-to-volume ratio. From statistical mechanics, the compactness factor minimizes Gibbs free energy, and the largest surface-to-volume ratio maximizes entropy. On this configuration, thermodynamic processes minimizing free energy are favored. In our model, we assume that the triangular grid is a natural mesh for all spacetime manifolds. Each vertex may or may not be occupied by a single quanta depending upon the population density. The probability of vertices occupancy may be as low as  $10^{-124}$  in the empty space or  $10^{-17}$  in a fermionic manifold (Table 1).

In a "crystal-like" lattice universe and for Planck energy close to a Brillouin zone the uncertainty on position and momentum vanishes [15]. By construction, individual quantum of one-unit lifetime  $t_P$  has no inertial mass and no momentum. Thus, quantum entities are massless motionless classic point events of a Minkowski spacetime. We view spacetime as a fabric of physical

quantum objects with variable density. The quantum population  $P$  of a region is linked directly to the action from

$$S = Ph = h \sum_j P_j \quad (2)$$

where the sum is carried over all vertices  $j$  of the tetrahedral lattice (Figure 1b). By analogy to the Thomas–Fermi electronic density model [16, 17], the quantum population density  $\mathcal{P}$  is also related to the Lagrangian and the action density at the Planck scale through  $\mathcal{S} = \mathcal{P}h$  and

$$S = \sum L t_P = \sum \mathcal{L} \ell_{Pt}^3 = \sum \mathcal{L} \mathcal{V}_P = Ph \quad (3)$$

and

$$\mathcal{L} = \frac{P}{\sum \mathcal{V}_P} h = \frac{P}{\mathcal{V}} h = \mathcal{P}h \quad (4)$$

where  $\mathcal{L}$  is the Lagrangian density. The density of action in continuous carrier fields as a primitive concept to all other physical quantities has been used to unify spacetime – action geometry and to derive GR and electromagnetism from a common ground [18]. Here, the spacetime-action field is made of finite discrete entities with density varying over more than 124 orders of magnitude (Table 1). From two-state  $\pm h$  quantum oscillators, kinetic and potential energy can be written as in QM in a similar way to Density Functional Theory (DFT) approach used in computational chemistry [19].

From Noether's theorem, the total population of a closed system<sup>7</sup> must be conserved, and a quantum current exists, as a poset of quanta in both directions along the time axis. Here, the notion of current does not imply continuous motion as in classical physics, but rather a stochastic spread of quanta in a static spacetime manifold. The conservation of the number of quanta is equivalent to energy conservation, but it implies also conservation of the total "number of quanta"  $P$  in the closed universe. A simple scale analysis indicates that our observable universe can be estimated to have a fixed total population<sup>8</sup> of  $P_U = M_U c^2 t_P / h \sim 10^{60}$  quanta at every Planck time slice. It is a remarkably small number of quanta at every instant. As illustrated in Table 1, the local population density is strongly modulated by the local mass ratio  $\mathcal{P}_j = \bar{\rho}_j / E_P$  of mean local mass density  $\bar{\rho}_j$  to the Planck energy  $E_P$  in region  $j$ . It ranges from 1 (Planck units in Table 1) at saturation to  $10^{-124}$  in lean regions of the universe, to about  $10^{-97}$  in Earth's environment and for atoms, or  $10^{-79}$  for protons and BH volume at the event horizon. The quantum density can be interpreted as a probability that any vertex of the grid (Figure 1b) at any Planck time be occupied by one quanta. It is noteworthy

<sup>7</sup> The whole universe or any single particle between two interactions (classical) points (exclusively) form a closed system.

<sup>8</sup> Comparable to the Hubble constant, the age, the mass and the diameter of the universe in Planck units.

for mention the similarity of quantum density between BH and proton near  $10^{-79}$ , suggesting that the quark volume confinement and asymptotic freedom may be related to the limit imposed on quantum causality as in BH. We note also the vast range in quantum population density of about 148 orders of magnitudes between Planck scale and laboratory scale where it becomes for all practical purpose a smooth quantum field consistent with classical field theories. The fixed total quantum population and the quantum dilution during inflation alleviate the vacuum catastrophe problem from other field theories and keep the cosmological constant at a level consistent with observation.

Since the total quantum population and the energy of a closed system are conserved, no energy is lost and the expansion or contraction of spacetime must be adiabatic and isentropic, as long as contraction of the universe would return the system to the initial state, and re-expansion would generate a similar universe from the cosmological perspective. As a binary system, the Qbit entropy  $\Sigma = P \log_2 2 = P$  is the net population  $P = \int d\mathcal{P}$  or  $P_o = m_{\chi_o} \ell_p^2 / \hbar t_p$  for a particle  $\chi_o$  of rest mass  $m_{\chi_o}$ . Hence in a closed system, this model assumes a constant total entropy proportional to the quantum population. The momentum of a particle can change only by discrete variation in quantum population.

In Malthusian population [20] dynamics, the regional population growth or decay rate at each Planck time step  $t_p$  is proportional to the current population density (number of individual per available cell locations within a region), but from finiteness, in a Verhulstian [21] dynamics, it is also proportional to the remaining available inoccupancy fraction

$$\delta P = rP(1 - P/P_{sat}) t_p \tag{5}$$

where  $r$  is the net local quantum regeneration rate. Without loss of generality, (5) can be scaled to

$$P'_{t+1} = rP'_t(1 - P'_t) \tag{6}$$

where  $P'_t$  is now the fraction of a saturated population at time location  $t$ . To account for quantum phase parity, a complex variable is introduced

$$\psi_t = P'_t e^{i\theta_t} / P'_o$$

such that

$$\psi_{t+1} = r\psi_t(1 - \psi_t) \tag{7}$$

where  $P'_o$  is some total population characteristic of the object and scaled such that the integral of  $\psi_t$  over the volume is properly normalized.  $\psi_t$  is a complex density function of a two-state system of oscillators with an amplitude of  $\pm 1$  associated to a discrete gauge factor having

$$\theta_t = (2t + 1)\pi/2, \quad t = 0, 1, 2, \dots, N.$$

In the continuous limit where  $P$  is very large, we have

$$\frac{\partial \psi}{\partial t} = \hat{r}\psi(1 - g_o\psi) = \hat{r}(\psi - g_o\rho) \tag{8}$$

where  $\hat{r}$  is generalized to a complex non commutative operator representing the local quantum regeneration rate,  $\rho = \psi^*\psi$  and  $g_o = P'_o/P_{sat}$  is a coupling constant ranging between 1 and  $10^{-124}$  in our universe depending upon the scale under consideration.

The generalization  $r \rightarrow \hat{r}$  of a scalar number to an operator is required since all observables are emerging properties from structures (gradients, Laplacian, lattice, etc.) in the quantum population distribution, as in QM.  $\rho = \psi^*\psi$  is a phaseless (real) quantum population density or a quantum probability for an interaction between two quanta of opposite phases (e.g.  $he^{i\pi/2} \leftrightarrow he^{i3\pi/2}$ ).  $\rho$  is a subset of the whole quantum population where an interaction  $\psi^*\psi$  occurred.

In turn, this subset of  $\rho$  constitutes a population of new objects on its own. In other words, by collecting all  $\rho$  events as a group of self-replicating objects, we may apply the logistic equation (6) again to the new class of entities. To some extent, we may apply this equation to many classes of reproducible objects emerging from interactive assembly of basic entities, to a population of water molecules in a gas or to a population of stars within a galaxy, for instance.

In the quantum world, generally  $g_o \ll 1$  (Table 1) and

$$\frac{\partial \psi}{\partial t} = \hat{r}\psi \tag{9}$$

which is the Schrödinger equation for

$$\hat{r} = \frac{\hat{H}}{i\hbar} = \frac{-\hbar}{i2m}\nabla^2 + V(\mathbf{r}, t) \tag{10}$$

or the Dirac equation for

$$\hat{r} = \frac{1}{i\hbar}[-i\hbar c\vec{\alpha} \cdot \vec{\nabla} + \beta mc^2]$$

where  $H$  is the Hamiltonian,  $V$  is a background potential of the environment,  $m$  is the mass,  $\vec{\alpha}$  and  $\beta$  are the standard Dirac matrix parameters. The Klein-Gordon equation is obtained by assuming

$$\hat{r} = \frac{\sqrt{-\hbar^2 c^2 \nabla^2 + m^2 c^4}}{i\hbar} \tag{11}$$

and by squaring the operators on both sides of equation (9).

At the interface between the two regimes, equation (8) may be separated in a quantum and a classical contribution

$$\frac{\partial \psi}{\partial t} = \frac{\partial \psi}{\partial t} \Big|_{Quantum} + \frac{\partial \psi}{\partial t} \Big|_{Classical} \tag{12}$$

where the classical term is at decoherence sites. In terms of the conserved quantum population, we can have also

$$\frac{\partial P}{\partial t} = \frac{\partial P}{\partial t} \Big|_{Quantum} + \frac{\partial P}{\partial t} \Big|_{Classical} \tag{13}$$

In the population of  $\rho = \psi^* \psi$  entities, the phase dependency vanishes and the quantum term collapses. Seen from equation (8), at the Planck scale and near saturation  $P \rightarrow P_{sat}$ ,  $g_o \rightarrow 1$  and  $\rho \rightarrow 1$  the interaction probability is strong; the wave solution is suppressed in (8) and collapses to a classic observation. Then the quadratic term in (8) cannot be neglected and approaches the classical limit

$$\frac{\partial P h}{\partial t} = \frac{\partial S}{\partial t} = -H \quad (14)$$

where the complex variable and operator are Wick rotated to the real domain. At the particle-particle interaction site, the quantum phase vanishes, resulting in the classical action as a scalar. Equation (14) is the classical Hamilton-Jacobi equation (HJ) for a classic particle from which geodesics on Riemannian manifolds can be derived for GR. The general equation (8) is a quantum-classical relation, a wave-particle description and a quantum-gravity candidate where the coupling constant  $g_o$  determines the interaction strength (likelihoods of  $\rho \rightarrow 1$ ). The quadratic factor  $\psi^* \psi$  expresses the degree of saturation of the population density. It represents the interaction between two quanta where in general one quantum<sup>9</sup> may belong to the background environment  $\mathcal{E}$  of another particle manifold, thus in general

$$\frac{\partial \psi}{\partial t} = \hat{r} (\psi - g_{\mathcal{E}} \psi_{\mathcal{E}}^* \psi) \quad (15)$$

so the nonlinear term represents a decoherence process. It is destructive for the wave solution in a similar way as in the Lindblad master equation [30, 31]

$$\begin{aligned} \frac{d\hat{\rho}(t)}{dt} &= \hat{\mathcal{L}}[\hat{\rho}(t)] \\ \frac{d}{dt} \hat{\rho}(t) &= \underbrace{-i[\hat{H}', \hat{\rho}(t)]}_{\text{Unitary Evolution}} + \underbrace{\hat{\mathcal{D}}[\hat{\rho}(t)]}_{\text{Decoherence}} \end{aligned} \quad (16)$$

where  $\hat{\mathcal{L}}$  is the Lindblad operator<sup>10</sup>, resulting in a standard Liouville-von Neumann equation with a lamb shifted Hamiltonian  $\hat{H}'$  renormalized due to interaction with the environment [22]. The general equation (15) introduces decoherence explicitly in QM and QFT.

The added nonlinear term  $g_o \psi_{\mathcal{E}}^* \psi = \delta(\psi_{\mathcal{E}}^*, \psi)$  is a delta Dirac function, splitting quantum and classical worlds in our universe. To the extent that  $P_o$  approximates a volume as for causet, its strength varies widely between gravity and nuclear interactions, but it is expected to unify approaching  $P_{sat}$  in BH. Because of the saturation effect in (15), the QPoD model predicts that gravity must weaken at high quantum densities instead of

<sup>9</sup> Recall that each quanta is indiscriminate from a particle to another during coincident interaction.

<sup>10</sup> Not to be confused with the Lagrangian density.

diverging into a singularity as in GR. Ultimately, it can lead us to measurable effects and a verification of the model.

Normally derived from statistical mechanics, here the Fermi-Dirac (FD) or the Bose-Einstein (BE) population distribution are the real part solution of (15) (Wick rotated) and they may be compared as

$$\begin{aligned} \frac{P(v)}{P_{sat}} &= g_o |\Psi(v)| = \frac{1}{e^{H/hv \pm 1}} \\ n_i &= \frac{1}{e^{(\epsilon_i - \mu)/\tau \pm 1}} \end{aligned} \quad (17)$$

where time is replaced by the inverse frequency as a clock,  $n_i$  the number of particle in state  $i$  in FD or BE distribution,  $\tau$  temperature,  $\epsilon$  the energy and  $\mu$  the chemical potential. It is a remarkable fact that FD and BE population are solutions of the same general quantum-classical equation as QM, QFT and HJ. It leads also to the Planck function for quantum population of photons as a solution of QPoD. In the limit of high energy, the solution asymptotes to the Gibb's distribution of standard thermodynamics.

Interestingly, the general logistic equation (8) allows the existence of two kinds of particles with distinct structures. We will see later that it can be achieved for distinguishable unitary cells (tetrahedron in Figure 1b as fermion) or undistinguishable composite multi cells structures (the complementary truncated tetrahedron part in Figure 1b as boson particles).

Furthermore, equation (17) links directly dynamics to thermodynamics with the total energy  $\epsilon = H$ , the temperature  $\tau = hv$  and the chemical potential  $\mu$  obtained from the coupling constant  $g_o$

$$\begin{aligned} -\frac{\mu}{\tau} &= \left( \frac{\partial \sigma}{\partial N} \right)_U \equiv \left( \frac{\partial \Sigma}{\partial P} \right)_{\epsilon} \\ &= \ln \left( \left| \frac{P_{sat} - P_o}{P_o} \right| \right) = \Delta \Sigma |_{P_o}^{sat} - \Sigma_{P_o} \end{aligned} \quad (18)$$

where  $P_o$  is here the total quantum population of a particle,  $U = \epsilon$  is total energy,  $\sigma$  the standard thermodynamic entropy and  $\Sigma$  the local quantum entropy of the population number  $N \equiv P$ . Another interesting result from (8) and (10) in the classical regime ( $g_o \approx 1$ ) when  $S$  is constant in (14), then  $r\rho = 0$  one finds expressions for inertial masses in terms of quantum entropy in Schrödinger or Dirac frameworks respectively as

$$m_s = \frac{\hbar^2}{2k_B} \frac{\nabla^2 \Sigma + (\nabla \Sigma)^2}{V} \quad (19)$$

and

$$m_D = \frac{i\hbar}{ck_B} \beta \vec{\alpha} \cdot \vec{\nabla} \Sigma$$

where  $\Sigma(\mathbf{r}, t) = k_B \ln \rho$  is the local entropy density for equally probable binary oscillators,  $k_B$  is the Boltzmann constant,

$$\nabla^2 \Sigma + (\nabla \Sigma)^2$$



are contributions of potential and kinetic energy to the inertial mass, and  $\nabla^2\Sigma$  is the spacetime quantum field curvature in terms of entropy. The quantum population field plays a similar role to the Higgs field of the Standard Model. In Schrödinger's framework, curvature in the quantum density field is responsible for the rest mass. Increasing the momentum also increases the density and the internal quantum potential. The external potential  $V$  from the environment is made of the superposition of all surrounding particle manifolds. When  $V$  is large, the quantum population density becomes large, the curvature flattens out and the inertial mass decreases. Conversely, as  $V$  approaches zero, in a lean environment, decoherence is rare, the classic reference frame is vanishing, and motion is hardly detectable, which would appear as increased inertia to a classic observer. Equation (15) states that the most likely location where decoherence occurs is in densest population regions. This is equivalent to the principle of least action leading the classical motion path as a succession of decoherence interactions within the environment.

### 4 Particle Structure

The most compact geometry maximizing the energy density in 3D is a tetrahedral cell (Figure 2a). However, to fully tessellate flat space a composite truncated tetrahedron (TT) (six basic tetrahedra + four octahedra) plus one simple tetrahedron (ST) are required. Together, the pair (TT + ST) forms a compact 3D space filling unit. ST has a dual cell (DT) with respectively opposite faces to each other. Further, the octahedron is composed of an interlaced pair of tetrahedra (ST + DT). Thus, the most fundamental cell in the grid forming a compact quantum population (Figure 1) in this model is a tetrahedron. The natural geometries of quantum manifolds may be constructed by equilateral triangles (2-simplex) as in CDT method of [12].

The elementary objects forming with tetrahedral cells may be categorized in two broad types: single cells (ST or DT in Figure 2c) and composite cells (TT in Figure 2b). The composite TT with radius  $1\ell_P$  and the elementary ST with edges  $\ell_P/2$  ( $\sim$ radius) are tentatively associated to boson ( $1h$ ) and fermion ( $h/2$ ) topology. In QPoD, they are particles of spin 1 and spin 1/2 respectively. The distinction of two categories has profound effects on allowed solutions. On any quantum manifold of particles, to satisfy unicity at most two fermion cells of opposite spin can coexist distinctively, ST and DT. Otherwise, because the oscillation modes of the whole manifold define the particle properties in spacetime<sup>11</sup>, there would be conflicting identities within that spacetime "patch" region. In other words, the resonance mode of one particle manifold can only support the properties defining

<sup>11</sup> This may be visualized as a 3D analog on spacetime to a 2D hologram in space.

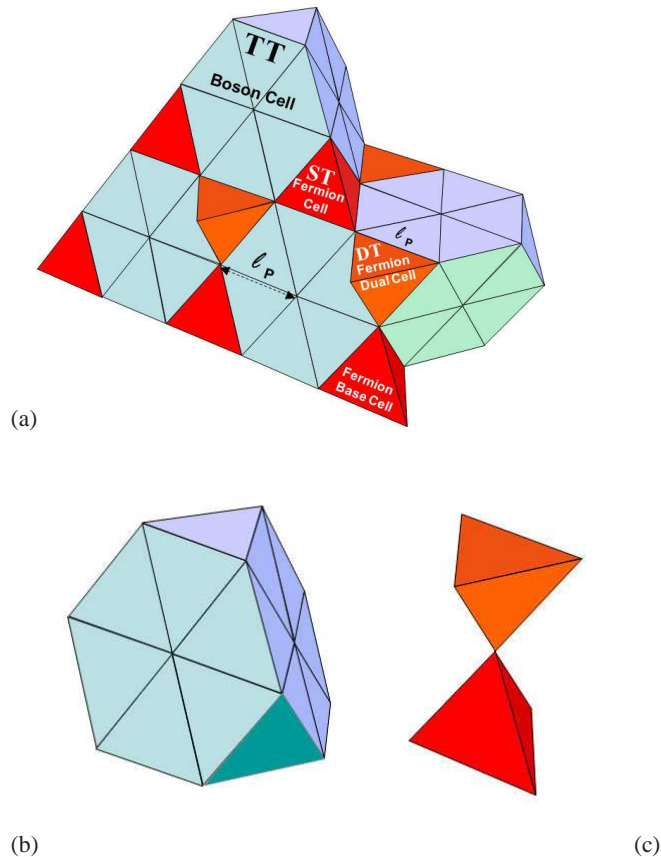


**Fig. 2** (a) Identification of TT and ST + DT cell elements from Figure 1 and isolation of (b) bosonic cell (TT) and (c) fermionic cells (ST + DT). The square of the volume ratio  $[(ST + DT) / TT]^2 = 1/132$ .

a single fermion in a given spin state without ambiguity. The dual DT cell allows for a second identical fermion with opposite spin only. The QPoD model naturally leads to a geometric origin of Pauli's exclusion principle in its fundamental structure.

As simple Platonic volume ST and DT cells have important properties. As mentioned, it is a self-dual figure leading to Pauli's exclusion principle. Furthermore, if we measure the spin state of particles in a Stern-Gerlach experiment, the projection of the spin in any orientation always leads to one of either  $\pm h/2$  along any arbitrary direction (x, y, z) independently. This property conforms well to experimentation.

Also, it is noticeable that the geometry of space defining elementary particles in this model have close similarities to geometry of sates and symmetries commonly encountered in particle physics [29]. This may not be surprising since in both cases the number of configurations is driven by the available site and modes defining all possible structures. So one might expect that

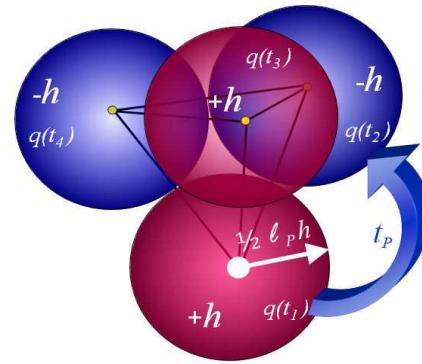
the symmetries observed in particles state is reflecting their internal structure to a good degree as the model suggests.

On the opposite to ST and DT cells, the composite TT cells permit many equivalent configurations and a large number of bosons to be in the same state. Hence the Bose-Einstein distribution of occupation. Multiple configuration of composite cells is the only physical way that the number of boson particles can exceed the saturation of elementary triangular loops (spin). In other words, to make physical sense, it is essential that the  $(e^{H/\hbar\nu} + 1)$  factor in the denominator of equation (17) represents numerous accessible configurations of a large set of elementary objects (spin loops) where by construction, the number of composite arrangement (entropy) possible exceeds the population of elements ( $P > P_{sat}$ ) in the logistic equation.

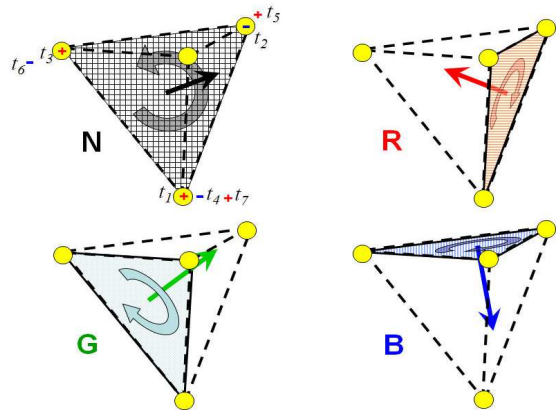
Recall, we make the hypothesis that elementary particles are resonance modes of independent quantum population manifolds (bubbles or patches of spacetime formed during inflation by a second quantization and constrained by causality). From translation symmetry on the lattice, we further postulate that it suffices to consider only a single compact 3D cell (as a particular case) to determine the physical properties of elementary particles that the 4D manifold may sustain. More generally, a resonance mode is a global property of the whole manifold and a great many “equivalent” configurations are possible. So for simplification, we limit ourselves to examine the properties associated with a single cell as one possible occurrence among many potential cases. It is just the simplest case possible and the easiest to interpret by geometry.

Circulation of quanta on any triangular face (Figure 3a) can be produced by a discrete wave<sup>12</sup> as a succession of alternating quantum states  $(+h, -h)$  occurring along the triangular loop, producing spin and helicity in the time direction. In the model, the spin is an angular momentum resulting from a discrete circulation of quanta on a closed loop<sup>13</sup> with discrete radius  $(1/2, 1, 2, \dots)$  times the action charge  $h$ . The smallest loop is the face of ST cells with spin of  $h/2$  corresponding to fermion particles. The next spin level is  $1h$  corresponding to bosons. Particle with spin  $2h$  and larger are possible. The circulation of alternating  $\pm h$  around one triangular face, forms an anti-symmetric  $\{+ [- + -]_{2\pi} [+ - +]_{4\pi}\}$  spinor with  $4\pi$  symmetry. Conversely, the circulation on the loop around a boson TT hexagonal face has a  $2\pi$  symmetry  $\{+ [- + - + - +]_{2\pi}\}$  in agreement with boson spin.

On each cell, a spin or a spinor can assume any of the four directions corresponding to each face of the tetrahedron (ST, DT or TT in Figure 3). Here, spins are constructed objects following a spin population dynamics



(a)



(b)

**Fig. 3** a) Structure of the fermion ST cell and b) the accessible modes of the spin loop on the cell. Quantum spin loop circulation on ST cell has 3 independent color charges  $\{R, G, B\} = -N$ , a neutral grey linearly dependent on  $\{R, G, B\}$  base color states. Reversing the loops, changes the spin, the charge and colors to anti-colors  $\{\text{Cyan, Magenta, Yellow}\} = N$  with reversed charge sign corresponding to antiparticles. Combining opposite spins in doublets or triplets cancel out the net spin  $\{RC, GM, BY, -NN\} = 0$ . All other spin combinations follow color theory.

of the logistic equation (8) on their own. The spin can take one of four modes depicted in Figure 4, ranging from a fixed orientation, to spin oscillation in 1D, to simple precession around any vertex or 3D chaotic circulation<sup>14</sup>. All of which are known solution of the logistic equation [3]. In general the logistic equation, applies to many reproducible object from atoms to macroscopic systems. However, the increasing complexity of interactions with scale renders the logistic equation a less exact approximation. On a single cell, only a small number of distinct spin states is accessible on the ST and TT cells. Each one is associated to the 12 known fermion particles of the Standard Model as summarized in Figure 5. Particles are normal modes of oscillation of spacetime manifolds made of quantum populations.

<sup>14</sup> Analogous to a three-body orbital trajectories for example.

<sup>12</sup> QPoD is somewhat similar to string theory and QLG with discrete oscillation on closed 2-simplex loop.

<sup>13</sup> Similar to closed strings in string theory and to spin network in quantum gravity theory.

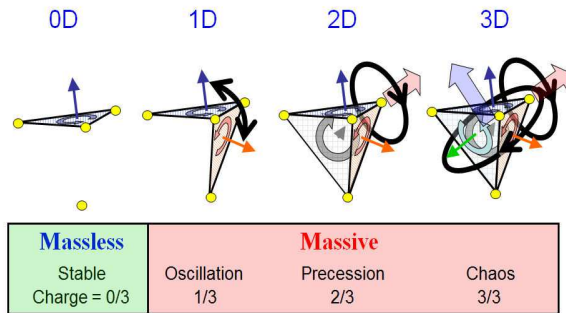


**Fig. 4** Spin modes on the tetrahedron cell. The model assigns rest mass to modes in 3D, electric charges to degrees of freedom or dimension of spin variation and color charges to the actual face occupied.

We hypothesize that the variation of the spin loop orientation corresponds to the electric charge and the direction of the spin { - inward, + outward } defines the sign of the electric charge, then the geometric properties of the model are isomorphic to fermions in the Standard Model. Anti-particles are obtained by reversing the spin handedness (parity) and the time direction (reversing circulation loops).

For instance, in our universe neutrinos are found always left-handed and antineutrinos are right-handed. From this model, we may speculate that during leptogenesis, with second quantization and symmetry breaking of time, normal matter and antimatter divided the classical universe (equation (8)) in two parts, where antimatter is evolving classically in the opposite time direction, as a possible solution for the problem of observed baryon asymmetry. In the alternate universe, classical time is going “forward” in the other direction, away from us but still towards their future and not our pass. There, neutrinos should be all right-handed and anti-matter follows the same physics rules as in our universe. This view is consistent with our model.

By addition of angular momentum, the sum of the opposite spins cancels out. The particular oscillation plane is the color charge {R, G, B} = -N then the model is isomorphic to the known fermion properties as illustrated in Figure 5. For a single quantum oscillating on ST faces  $f = \{1, 2, 3, 4\}$ , we define the basic family of the first-generation {v, u, d, e-} making ordinary matter. Only four generations of similar particles can be produced by populating vertices of the ST or SD cells by more quanta  $p = \{1, 2, 3, 4\}$ . The first three modes  $p = \{1, 2, 3\}$  generates all the known copies of the first generation. In each generation, the charge properties are conserved, but

the action and the rest mass must increase according to the quantum population density.

Similarly, one can infer that bosons formed on TT cells are in some way like in supersymmetry, by TT SD symmetries, to each fermion correspond a boson in terms of structure. In QPoD, two classes of spin 1 boson dominates, matching with the lightest stable fermion, the electron-positron and the electron neutrino, they are the massive  $W^\pm$  boson  $(p, f) = (1, 4)$  and the massless photon  $\gamma$  with  $(p, f) = (1, 1)$  respectively. They are the two most likely occurrences for the same reasons of stability and minimum energy of their fermion counterparts. However, a detailed examination of bosons deserves more attention than intended in the current work. The QPoD model predicts the existence of a fourth generation of matter particles. However, by filling all 4 vertices and all 4 faces, only one new scalar particle can exist as a quad according to this model. As the single member of the fourth generation, we name this new particle “quatron.” Since all faces and vertices are occupied, the quatron has no spin, but its (ST + DT) structure must still follow FD statistics. Based on properties of other particles, we infer that it is chargeless and colorless, but a very massive matter particle. It has only two discrete orthogonal oscillation states (interchanging blue -h and red +h in Figure 3a). Being its own antiparticle, it is a Majorana type. Although not a fermion (spin  $nh/2$ ), but a spinless scalar<sup>15</sup>. Despite the absence of spin, the structure of the quatron is tetrahedral (ST + DT) geometry, unlike TT for bosons. As a compact structure with minimum Gibbs free energy, quatrons are expected to be stable<sup>16</sup>.

The electron is also stable with four faces occupied, but one vertex and a minimum quantum action. Quatrons have the characteristics often associated to weakly interacting massive particles (WIMP), with properties consistent with the hypothesized cold dark matter (CDM) observed in our universe.

## 5 Results

To verify the QPoD model against observations, we examine the relationship between measured masses of fermion and model geometry deduced from Figure 5. It is unlikely that would exist by chance alone, over such a broad scale of particles mass range, a simple relationship between observed masses with vertex  $p$  and face  $f$  occupancy, but it does. In Figure 7, we have plotted the graph of fermion energy as the log in base 2 of the mass<sup>17</sup> ratio with respect to that of a pair production electron-positron<sup>18</sup> taken as a reference from the

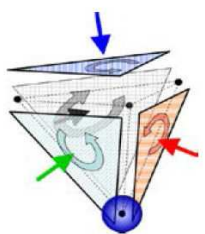
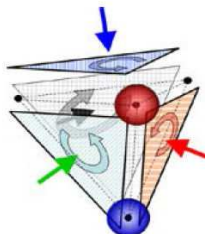
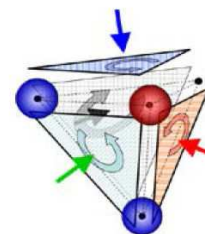
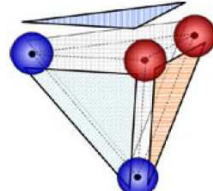
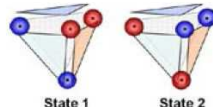
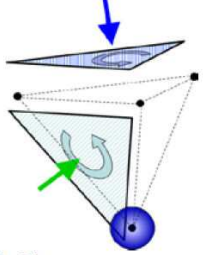
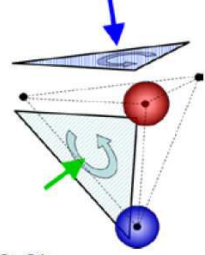
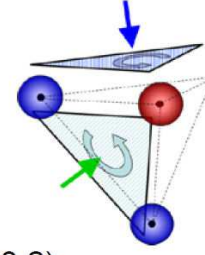
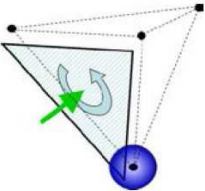
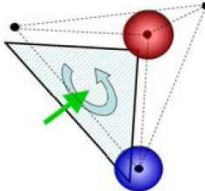
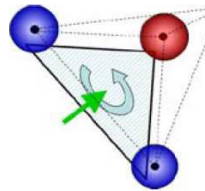
<sup>15</sup> Here, we distinguish spinless as “without any spin” from spin zero which may come from a “balance of existing spins”.

<sup>16</sup> By analogy to rare gas atoms with full electronic orbitals.

<sup>17</sup> For binary spin loop oscillators

<sup>18</sup> The reference to 1.022 MeV is arbitrary as other choice would shift the curves along the ordinate axis.



	I	II	III	IV
	Electron	Muon	Tauon	Quatron
Leptons (-3/3)	 $(1,4) = (p, f)$	 $(2,4)$	 $(3,4)$	 $(4,4)$
Quarks (+2/3)	Up Quark	Charm	Top	Very Massive No Parity Spinless Chargeless Colorless Majorana Two States  Stable
	Down Quark	Strange	Bottom	
Quarks (-1/3)	 $(1,2)$	 $(2,2)$	 $(3,2)$	
Neutrinos (0/3)	Electron Neutrino	Muon Neutrino	Tauon Neutrino	
	 $(1,1)$ (STABLE FERMION)	 $(2,1)$	 $(3,1)$	

**Fig. 5** Periodic table of elementary particles in QPoD model based on 3-simplex geometry with all possible occupancies of vertices  $p$  and faces  $f$ . The parentheses label the vertex and face occupation on the ST tetrahedral cell. Quantum oscillation ( $\pm h$ ) is produced on closed triangular loops as discrete waves generating anti-symmetric spin themselves oscillating on different faces  $f$ . Stable particles are highlighted in red. Based on 12 known fermions, the hypothetic quatron is a spinless scalar with a minimum degrees of freedom.



best-known minimum value of massive particles. The choice of the mass ratio avoids any reference to an arbitrary unit system. When converting mass into quantum population from equations (1) and (19), as a pure number and a measure of entropy, the diagram in Figure 7 is a relation of populations only<sup>19</sup>,  $m = m(p, f)$ . On the abscissa is the independent variable as the number of face occupations for each particle, i.e. the population of spins. The plot is repeated for the three generations ( $p$ ) of fermion families ( $f$ ).

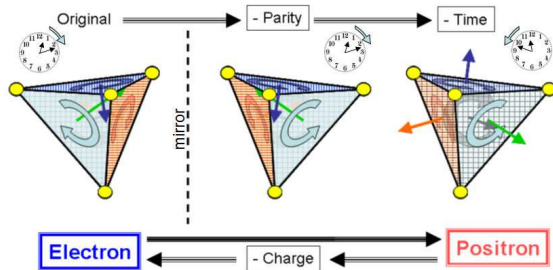


**Fig. 6** Illustration of CPT symmetry in QPoD model. All particle properties are invariant under combined inversion of Parity, Time and Charge. Conversely, an inversion of parity and time is identical to an inversion of electric charge. Anti-particles are particles that are evolving in the reverse time direction [24]. The same CPT invariance rule applies to all particles in the model.

The table of elementary particles and antiparticles from Figure 5 can be summarized on a matrix form as in Figure 8, where light particles (lepton sectors) are on the sides, and massive particles in the quark sector are in the central columns and in the lower row. Majorana type, with the particles being their own antiparticles, are identified from geometry in Figure 5. They are electrically neutral particles. In the model, Dirac's particles carry electric charges. Stable particles are located in relative minima of energy in the corners of the matrix.

The distribution of fermion masses spreads over more than 8 orders of magnitude, from the neutrino to the top quark, although the neutrino masses is only estimated as an upper limit from experimental data. From the graph, data follow approximately a parabola, which in itself is not surprising from only three points, but not obviously so symmetric. Further, the extrapolation to mu-neutrino and tau-neutrino agrees on very low masses there. In  $(p, f)$  coordinates, the figure 7 shows a simple geometric relationship with observed masses of all fermions. To investigate further that relationship, we fitted empirically the parabola on Figure 7. If the relationship has a physical

<sup>19</sup> Since the wave function is the normalized populations  $\pm\hbar$  and all observables are derived from them.

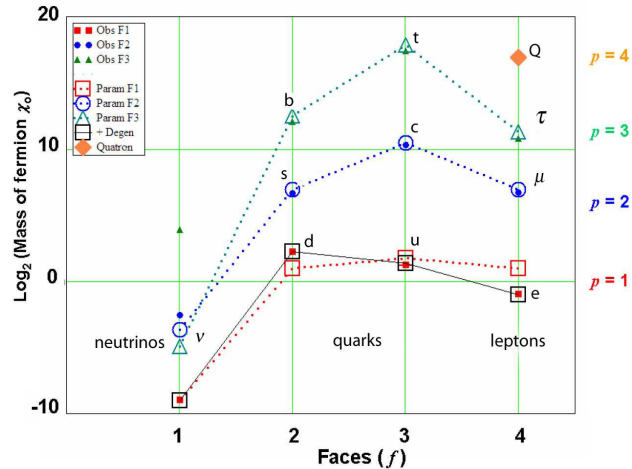


**Fig. 7** Elementary particle masses versus number of spin loop faces  $f = 1 \dots 4$  for each vertex occupation  $p = 1 \dots 4$ . The solid dots are “observed” values and corresponding open dots and dotted lines are parameterized from equation (20) without correction ( $\kappa = 0$ ), except for first generation (red lines  $p = 1$ ) where the black line includes the correction term  $\kappa$ . Value for  $e^-$  neutrino is prescribed, while for  $\mu$  and  $\tau$  neutrinos, it is extrapolated from (20). Antiparticles are identical, but with reversed spin direction. Stable particles  $\{v, e, Q\}$  have least action, minimum energy or full face  $f$  or full vertex + faces,  $p = f = 4$  ( $Q$ ). The correction  $\kappa$  is much smaller (not shown) for 2nd and 3rd generations.

$$\mathcal{F} = \begin{matrix} & \text{Face } f & & & \\ & \begin{matrix} 1 & 2 & 3 & 4 \end{matrix} & & & \\ \begin{matrix} 1 \\ 2 \\ 3 \\ 4 \end{matrix} \text{Vertex } p & \begin{matrix} v_e \\ \text{Lepton } \mu \\ \text{Neutrino } \nu_\tau \\ 0 \end{matrix} & \begin{matrix} d \\ s \\ b \\ 0 \end{matrix} & \begin{matrix} u \\ c \\ t \\ \text{WIMP} \end{matrix} & \begin{matrix} e \\ \text{Lepton } \mu \\ \tau \\ Q \end{matrix} \end{matrix} \quad \mathcal{F}^- = \begin{matrix} & \text{Face } f & & & \\ & \begin{matrix} 1 & 2 & 3 & 4 \end{matrix} & & & \\ \begin{matrix} 1 \\ 2 \\ 3 \\ 4 \end{matrix} \text{Vertex } p & \begin{matrix} \bar{v}_e \\ \bar{\nu}_\mu \\ \bar{\nu}_\tau \\ 0 \end{matrix} & \begin{matrix} \bar{d} \\ \bar{s} \\ \bar{b} \\ 0 \end{matrix} & \begin{matrix} \bar{u} \\ \bar{c} \\ \bar{t} \\ \text{Majorana} \end{matrix} & \begin{matrix} e^+ \\ \bar{\mu} \\ \bar{\tau} \\ \bar{Q} \end{matrix} \end{matrix}$$

$$\mathcal{F} + \mathcal{F}^- = 0$$

**Fig. 8** Matrix representation of matter particles and antiparticles according to QPoD model. Stable particles located in corners are marked in red color. Majorana and Dirac particles are determined by the symmetry between particles and corresponding antiparticles. Particles form definite sectors (labeled) in terms of their properties and geometry. Adding antiparticles to particles annihilates all spin, charges, action (locally) and physical quantum structures.

basis, one might expect that the fitted parameters would take a simple form such as natural numbers or special angles, and once again, it does.

By parameterizing empirically the mass ratio of particle  $(p, f)$  with respect to the mass  $m_{e^\pm}$  of a  $(e^-, e^+)$  pair (say 1.022 MeV) as reference in terms of the independent variables  $p$  (vertex) and  $f$  (face), we find

$$\log_2 \left[ \frac{m_{p,f}}{m_{e^\pm}} \right] = \underbrace{-C_p \varepsilon p}_{\text{Occupancy}} - \underbrace{C_p(2-f)(4-f) \sin[\pi/(8-2p)]}_{\text{SpinLoop Oscillation}} + \underbrace{\kappa_{p,f}}_{\text{Degeneracy}} \quad (20)$$

where  $p = [1, 2, 3, 4]$ ,  $f = [1, 2, 3, 4]$ ,  $\varepsilon = \ln(1/2)$  and  $C_p = [-\varepsilon^{-1}, 5, 6, 6]$ .

Remarkably, all fitted coefficients and parameters based on geometry alone are dimensionless natural numbers, except for the factor  $\varepsilon$  representing a change of logarithm bases between 2 and  $e$ . A minor correction factor  $\kappa_{p,f}$  is tentatively associated with a degeneracy  $D$  term for quantum states per cell configuration and fitted well by a linear correction on Dirac charged particles only (Figure 8)

$$\kappa_{p,f} = D_{p,f} a_p + b_p \quad (21)$$

where

$$a_p = (-0.538, 0.042, -0.62, 0),$$

$$b_p = (4.457, -0.548, 0.856, 0)$$

and

$$D_{p,f} = \begin{pmatrix} 0 & 6 & 9 & 12 \\ 0 & 6 & 9 & 8 \\ 0 & 2 & 3 & 4 \\ 0 & 0 & 0 & 0 \end{pmatrix}, \quad (22)$$

where  $p = [1, 2, 3, 4]$ ,  $f = [2, 3, 4]$ , but with no correction for Majorana particles,  $\kappa_{p,1} = \kappa_{4,4} = 0$  without degeneracy on faces from oscillation modes (Figure 5).

The states  $(p, f)$  produce 13 distinct configurations and each is compared to 12 known fermion particles plus one new matter particle of a 4<sup>th</sup> generation, designated as "quatron." In Figure 7, plotting the observed fermion masses as a function of  $f$  for groups of  $p$  (only dimensionless geometric parameters) produces parabolic distributions characteristic of the logistic equation (6).

Here, the unknown mass of neutrino is replaced by the maximum expected values. Yet, the  $\mu$  and  $\tau$  neutrinos extrapolated from (20) converge close to the upper limit of e-neutrino set to  $2^{-9}$  (or 0.002 MeV) in (20). The first term on the right hand side of (20) is due to the occupancy  $p$  (generations of fermions), while the second term is mostly from spin loop oscillation  $f$  (families), except for the projection factor  $-C_p \sin \vartheta_p$  where

$$\vartheta_p = \{ \pi/6, \pi/4, \pi/2, \pi \}$$

cancels out for quatron  $p = f = 4$  from the factor  $(4 - f)$  in (20). This is an indeterminate angle, but sinus function bounded to  $\pm 1$  consistent with the chaotic oscillation of that mode (Figure 4). It can be set to  $\vartheta_4 = \pi$  by symmetry. The results are summarized in Table 2 where the masses of fermions from QPoD model are compared to observed masses.

Equation (20) states that the mass ratios of elementary matter particles are a superposition of two distinct populations of objects, quanta occupancy (the first term on the right-hand side) and a population of spin loops expressed in terms of degree of freedom (the second term on the right-hand side). The last minor term seems to increase stability of the electron and quarks mixture. Not only QPoD model produces fermionic generations and families properly, but it fits the masses well with "natural numbers", an indication of a possible physical interpretation for this long-lasting puzzle. To investigate the links between (20) and the fundamental equation (6), we do a Poincaré recurrence map for the scaled variation of spin loop population on a ST cell. In the model, it is the variation  $\delta$  of spin loop  $\{R, G, B\}$  that modulates energy-mass and the electric charge, while each spin loop has a color charge according to direction such that  $\{R, G, B\} = -N$  neutral grey with corresponding anti-colors  $\{C, M, Y\} = N$  for reversed spins (antiparticles). One can verify that particles in this model are CPT invariant (Figure 6) and color symmetries are respected.

The logistic equation has been vastly studied [3, 25-27]. In the analysis of each generation, the maximum scaled population at  $P' = 1/2$  in Figure 9 is normalized on the ordinate axis to unity and  $\mu$  is varied to find fixed points. Apart, from the minor correction from the  $\kappa_{p,f}$  degeneracy factor, all fermion particles (Figure 10) have a corresponding fixed-point as possible solutions of (6) for the following  $\mu(f)$  values

$$\mu = \mu_f = \{0, 4, 6, 12\}/3$$

where  $\mu = 0$  for the neutrino is a super stable fixed point.  $\mu = \{4, 6\}/3$  (6 quarks) are stable solutions of equation (6), while for the other  $f = 4$  leptons of the  $\{e^-, \mu, \tau, Q\}$  family,  $\mu = 4$  is a known chaotic solution of the logistic equation. This is consistent with the expected modes depicted in Figure 4.

At this point, we may interpret the result expressed in figure 9 in terms of the initial equation (6) of the discrete model as follows. The Poincaré diagram compares in ordinate the population dynamics equation (6)  $P'_{t+1} = \mu P'_t (1 - P'_t)$  at an adjacent time step to the present state  $P'_t$  in the abscissa for different values of the regeneration rate  $\mu$  (dimensionless  $r$ ). Here the scaled population  $P'$  is not the quantum population *per se*, but rather the quantum spin loop (triangular faces) population as a secondary derived entity. As for Dirac equation, it is addressing the question of a possible relationship between spin population states at successive time steps (i.e. about a possible dynamical relationship following the logistic

**Table 2** Comparison of elementary particle masses (MeV/c<sup>2</sup>) between QPoD model from the equation (20) and experimentally observed values (bold and underlined figures) for each family and generations from Figure 5. A 4<sup>th</sup> generation WIMP scalar particle, the quatron (Q), is predicted by the model. In the current model, only the e-neutrino is prescribed to 2<sup>-9</sup> ratio (0.002 MeV/c<sup>2</sup>). The electron-positron is given for normalization of the dimensionless mass ratio as a reference.

QPoD / Observed**	1st generation p = 1	2nd generation p = 2	3rd generation p = 3	4th generation p = 4
1st family f = 1 (neutrinos)	0.002 / (<0.002)* ν <sub>e</sub>	0.08 / (<0.17)* ν <sub>μ</sub>	0.02 / (<15)* ν <sub>τ</sub>	104000 Q (scalar)
2nd family f = 2 (d, s, b)	4.8 / <u>3 to 7</u> d	101.6 / <u>95 ± 25</u> s	4464 / <u>4450 ± 320</u> b	
3rd family f = 3 (u, c, t)	2.6 / <u>1.5 to 3</u> u	1286 / <u>1225 ± 90</u> c	186000 <u>174200 ± 3300</u> t	
4th family f = 4 (e, μ, τ, Q)	0.511 / <u>0.511</u> e	107.7 / <u>105.7</u> μ	1890 / <u>1777</u> τ	

\* Estimated maximum value

\*\* Yao et al (2006) [23]

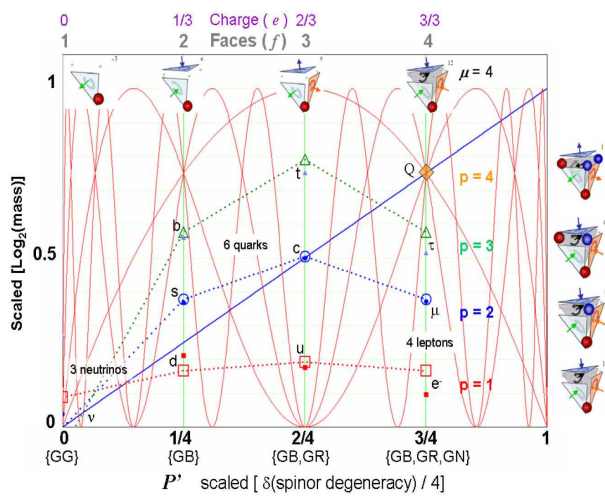


**Fig. 9** Poincaré iteration map for particle mass ratio with a fixed points for Figure 7 with  $\mu = 4$ . The first 4 iterations are shown as solid red lines. Solid small dots are observed particle masses and open dots with dotted lines are from equation (20) without the  $\kappa$  correction. Only the solution for  $(p, f) = (4, 4)$  is shown. Other solutions (Figure 10) are found after renormalization of the maximum center to unity and varying  $\mu$  in the  $[0, 4]$  range to find each solution. Icons show cases for 13 different configurations of  $p$  generations and  $f$  families. The abscissa is the degeneracy of color variations (Figure 4) seen from any one spin loop reference point, as exemplified by {GB, GR, GN} for the Green face case. The predicted quatron scalar particle is shown as an orange diamond.

equation for this case). On ST (or DT) cell, only the 13 distinct configurations identified are possible. The measurements show that 12 observed fermion masses are consistent with such a relationship. There is correspondence between masses and associated fixed points of spin loop states in spacetime geometry at the Planck scale. Recalling that according to the masses relation in Schrödinger representation  $m_S$  of equation (19) and for a particle at rest, the mass is proportional to the Laplacian of the quantum entropy  $\Sigma$  or to the log of the population (or the log of probability) and the diagram in Figure 9 is basically a scaled population – population map at different time levels (orders of iteration).

The model suggests that neutrinos with a fixed spin direction are super stable solutions with their Laplacian vanishing in one particular direction, but not in the spin plane (Figure 5). In the direction without a Laplacian contribution, the particle mass vanishes, allowing for propagation at the speed of light (the grid mesh) in that direction alone. The neutrino’s manifold stretches out in the one direction that we observe, after decoherence in the environment, as the direction of motion. The virtual motion is perpendicular to the spin plane and results in the helicity of neutrinos. Although not discussed here, a similar situation occurs on the TT cell (spin 1 boson) corresponding to the photon manifold structure. Essentially, particle modes confined to one spin loop plane are massless in one direction and seen as propagating at the light speed in that direction. However, their non-vanishing Laplacian in the spin plane imposes inertia to change of direction, leading to scattering, refraction and diffraction optical properties or acceleration in a gravity field.



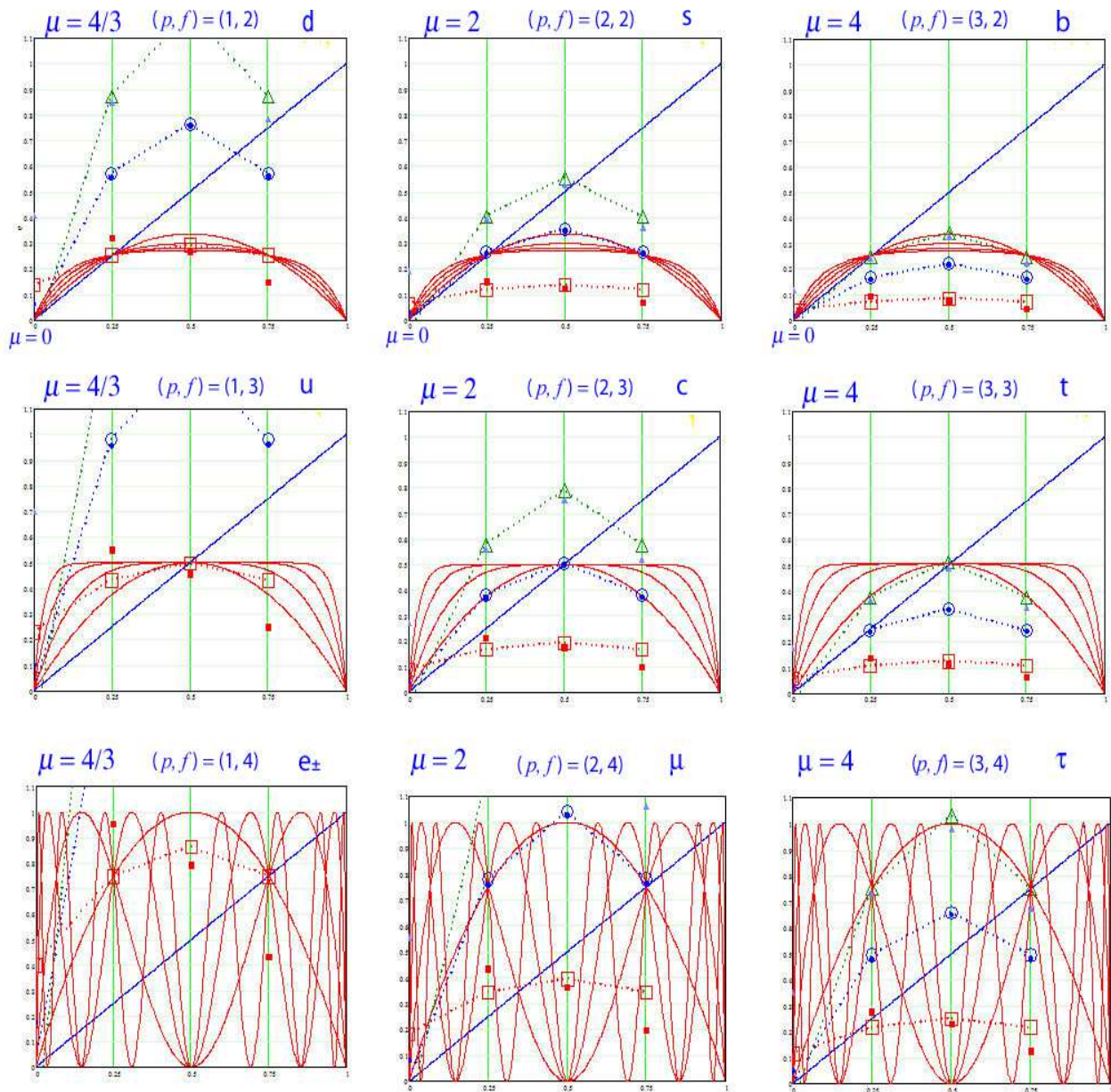


**Fig. 10** As in Figure 9, but for other massive fermions. It is obtained by normalization to the  $f = 3$  maximum masses of each generation  $p$  respectively and varying  $r \equiv \mu$  to fixed points from equation (6). The fixed points for neutrinos are found with  $\mu = 0$ . The red lines are the first 4 Poincaré iterations showing the range of possible stable, oscillatory and chaotic solutions to the logistic equation (6).



All other spin modes in 2D and 3D have Laplacian contributions in every direction and according to (19) they must experience inertial mass as a scalar quantity. Figure 9 shows that observed masses of fermion correspond to fixed point of the Poincaré map of the logistic equation (6). It also explains the maximum mass of top and charm quarks in their respective generation. As the spin loop occupancy on ST (DT) cells moves to 4 faces, the result is a local minimum of energy and a relative decrease of the particle mass in their respective generation. At both ends of the mass curves, leptons can form stable particles for different reasons. One is the local minimum mass (electron and e neutrino) and the second is the full face occupation with a local minimum energy. Muon and tauon with partial vertex occupation are expected to decay toward electron and neutrino minima. Particles with 4 faces are colorless since all 4 faces are equally probable. The exception in terms of stability, might be a quatron particle with complete faces and vertices occupied by quanta as a third stable structure. In that model, quarks must be combined to form stable colorless particles with resulting 4 faces effective occupation in a wide range of possibilities, e.g. forming hadrons.

The departure of the model masses from quadratic relation is interpreted as a consequence of multiple state degeneracies, which is largest in the first generation (normal matter) due to one quantum with several accessible vertices and spin loops. The degeneracy is maximal for the electron, increasing its stability. It is thought as being a possible cause for a reversal in up – down quark mass with respect to other quarks. The contribution of degeneracy decreases with mass as the cell fills up occupation with fewer alternate configurations accessible.

By filling all vertices, the mass of the quatron particles ( $p = 4$ ) is independent of  $f$  and equation (20) reduces to the leading occupancy term

$$m_Q = m_{e\pm} 2^{-C_p p E} \tag{23}$$

which, using our parameterization (20), is approximated by extrapolation to a mass of about 104 GeV, close to the recently found Higgs boson (125 GeV). In fact, a value of  $C_p = 6.097$  instead of  $C_p = 6$  would correspond more accurately to the Higgs' mass. Only one particle is missing for completing the table from the Poincaré map, it is the single member of a fourth generation previously introduced. It is a spinless particle with properties similar to that expected for the WIMP as a candidate for dark matter in cosmology. Filling ST vertices  $p$  and faces  $f$ , minimizes the action owing for stability and neutralizes all charges, allowing only for weak and gravitational interactions. Since the expected mass of the new quatron is close to the recently found Higgs boson, we may wonder if the particle found at 125 GeV could be the illusive CDM/WIMP particle responsible for the observed dark matter.

Another result from the model concerns the interpretation of the nature of interactions and forces. In

QPoD, accelerations (and forces) are generated when decoherence (equation (15)) occurs in a background environment having a quantum population gradient density  $\nabla \psi_{\mathcal{E}} = \nabla (P_{\mathcal{E}} e^{i\theta_{\mathcal{E}}}) / P_0$ . Because the probability of interaction of a particle with the environment is function of the combined amplitude density ( $\psi_{\mathcal{E}}^* \psi$ ), it is most likely to occur down the gradient where ( $\psi_{\mathcal{E}}^* \psi$ ) maximizes, hence acceleration of observed motion and an apparent entropic force in the direction of the quantum population gradient. The strength of the interaction depend on the product ( $g_{\mathcal{E}} \psi_{\mathcal{E}}^* \psi$ ) where the coupling constant  $g_{\mathcal{E}}$  is dominated by the change of scale cause by the interaction and collapse of the wave function. For instance, the coupling constant  $g_{\mathcal{E}} \sim \mathcal{P}_{ST+DT} / \mathcal{P}_{TT}$  in (15) in electromagnetic interaction of a photon with an electron is close to the volume ratio (fermion to boson)  $[(ST+DT)/TT] = 2/23$  in Figure 2b) and 2c), The fine-structure constant  $\alpha$  can be estimated by the volume ratio  $[(ST+DT)/TT]^2 = 1/132$ , thus

$$g_{\mathcal{E}}^2 \sim (\mathcal{V}_{fermion} / \mathcal{V}_{boson})^2 \sim 1/132$$

near the known 1/137 ratio and median to the 1/127 value observed at the Z boson scale. Similarly, the coupling constant of fermion – fermion strong interaction in quarks is of order one, while at the other extreme, gravitational particle to background interaction (Table 1) must be very small at a human scale. For instance, the gravitational interaction of a proton in Earth's environment is about

$$g_{\mathcal{E}}^2 \sim (\mathcal{P}_{proton} / \mathcal{P}_{Earth})^2 \sim 10^{-36}$$

or at the scale of the solar system environment

$$g_{\mathcal{E}}^2 \sim (\mathcal{P}_{proton} / \mathcal{P}_{Solar\ system})^2 \sim 10^{-44}.$$

At very high energy densities, approaching the Planck scale, the model shows that all interactions should converge to unity since  $(g_{\mathcal{E}} \psi_{\mathcal{E}}^* \psi) = 1$ . In some sense, the coupling constant of the model represents a densification or a dilution of the action density during change of scales by conserving energy while changing volume and action density.

## 6 Conclusion

In an attempt to understand the observed properties at the quantum scale and searching for a possible link with classical physics, we investigated a model based on the logistic relation common to many problems involving population of selves-replicating objects. Our application of the nonlinear logistic to quantum dynamics is proposed as a way to explore the Planck scale topology of elementary particles, their properties and their interactions. Still very tentative and exploratory, at times speculative, aimed to promote discussions, the proposed conceptual framework is rich in potential solutions to several fundamental problems in contemporary physics.

Perhaps the strength of this simple approach is the naturalness of interpretations without appealing to unseen physics like extra dimensions and multiverse or relying on a default anthropic principle. Far from a complete theory, we think that QPoD is a domain of research that needs to be studied more rigorously with the hope to resolve some of the most pressing issues in current physics. To this end, what has been learned already by observing our micro environment over more than a century starting with Planck's work [28] is highly inspiring.

The extension of the usual quantum definition as the smallest quantity of any field to that of a finite 4D physical entity with unitary extension and intensity of one Planck length diameter and one unit of action with two states ( $\pm h$ ), has profound consequences. Based on natural units, the model needs no constant *a priori* nor pre-existing variables to construct physics as we know it from observation. Hypothesizing that quanta are causal, finite and conserved entities, we infer that the non-overlapping and self-replicating quantum object forms unique compact structures. It is a natural lattice grid whose geometry is isomorphic to elementary particles of the Standard Model.

With a constant total quantum population, the universe modulated by quantum clusters is nonetheless constrained to follow causal rules. Modeled on the behavior of population dynamics, the logistic equation describing the most probable states is explored as a possible quantum-classical relationship. In a background independent system, spacetime emerges has a 4D distribution of static quantum entities coexisting at once, that can be approximated by a continuous manifold on the scale much larger than the Planck scale (say  $10^{-20}$  to  $10^{+26}$  meters or  $10^{-30}$  to  $10^{+16}$  seconds) where any measurements are done. In this context, the time dependency is not an evolving population in one particular time direction as in classical physics, but rather a most likely population distribution forming spacetime itself, each occurrence being one particular solution of the dynamics. The regeneration rate of the population is taken as the local energy (Hamiltonian) divided by a quantum unit of action. By suitable choice of local quantum population growth rate, the standard Schrödinger (quanta) and Dirac (spin) equation are fully recovered and both theories (QM and QFT) are respected when the population densities are far from saturation. This condition of linearity is verified to a very high level for normal conditions of quantum densities found within the universe. However, it is violated at very high-energy densities where the logistic equation saturates and the local variation of the population levels off.

In the linear regime, at very low population number density and to maintain causality, the model suggests that individual particles should be created in a second quantization process of spacetime. These particles are normal modes of broken patches of quantum population. They form nearly independent 4D manifolds of quanta, overlapping with very low probability of interaction.

When two manifolds interact by rare conflicting collocation at one site, the quadratic term of the logistic equation reaches 1 locally, and the wave function solution collapses into a classical observable information (location, momentum, mass, charge, etc.) for a brief instant of one Planck time. Then time symmetry is broken at the interaction location. The subset of all interaction locations forms our observed classical space and follows the Hamilton-Jacobi equation and classical thermodynamics. The interaction process at the quantum-classical boundary can account for the observed decoherence phenomena. Depending on parameters, the solution of the QPoD equation can be a quantum population state of the types Fermi-Dirac, Bose-Einstein or Gibb's distributions at higher energies. The statistical mechanics solution from the QPoD equation permits to identify key thermodynamic variables: temperature, free energy, entropy and chemical potential. As a result, the mass of particles and momenta can be expressed as variation of quantum entropy or curvature of the quantum field, a potential in analogy to the Higgs process. During particle-particle interaction or approaching singularity in BH or at beginning of the universe prior to inflation, when quantum density approaches unity, all derivatives (Laplacian, gradient or time derivative) tend toward zero in a flat field, but the chemical potential increases. When the chemical potential exceeds the free energy Hamiltonian, then the population state is unstable, leading to adiabatic expansion of the manifold, accounting for spreading out of the wave function and the inflation in the early phase of the universe.

From its unique compacted structure and in support to the quantum population dynamics model, we investigated the link between elementary ST or DT spacelike cells and fermion properties. The Heisenberg uncertainty and Pauli's exclusion principles are naturally accounted for by the model. It is found that the compact cell geometry leads to antisymmetric spin loops on ST faces. The variation of the spin direction follows electric charges of fermions, while the actual face occupation follows the color charges of particles. Anti-particles are obtained by reversing handedness and time. CPT and color symmetries of the Standard Model are respected. The map of face and vertex occupation on ST (DT) cell gives us a periodic table of fermion with proper families and generation of particles having identical charges, but different masses. The relationship between masses and ( $p, f$ ) vertices-faces oscillation modes derived empirically results in a simple equation where independent variables ( $p, f$ ) and coefficients take simple values, natural numbers  $\{1, 2, 3, 4, 5, 6\}$ , projection angles  $\{\pi/6, \pi/4, \pi/2, \pi\}$  and base change  $\{\ln 1/2\}$ . Considering that in a power law taken over about 8 orders of magnitude is sensitive to parameters and expecting that a fundamental TOE would only require dimensionless natural numbers, although not a rigorous proof, nevertheless, these results are very encouraging. The simple fit is not perfect as a small correction factor needs to be introduced. This correction

is interpreted as an artifact of quantum degeneracy dominant in the lower modes of ordinary matter.

Another strength of the model is the parabolic relationship between masses and independent variables ( $p, f$ ) which is consistent with the logistic equation as seen from a Poincaré map. By scaling the mass diagram, we find that each particle mass has a possible fixed-point solution. Consistently, with the spin modes on ST cell (Figure 4), the fixed points of the Poincaré map are super stable for neutrinos, stable modes for quarks and chaotic oscillations modes for the other leptons.

Perhaps the most intriguing result is the prediction by the model of the existence of a new particle as the single member of a fourth generation. Named quatron, this particle results from filling completely the vertices and faces of the ST (DT) cells. The result, interpreted based on 12 other known fermion modes indicates that quatron is a massive scalar particle, spinless, chargeless, colorless with only two orthogonal states. By minimizing Gibbs free energy, filling all possible occupations, the new particle is hypothesised to be very stable. Quatron is a scalar field that could be a viable candidate for the illusive CDM particle. Its mass is estimated near 104 GeV, close to the recently discovered Higgs' boson.

Just hypothesizing the existence of a conserved quantum entity with unitary 4D extension ( $\ell_P, t_P$ ) and a dual state intensity of action  $\pm h$  leads us to a unique compact lattice baring the essential properties of elementary particles. QPoD model proposes a physical composition for spacetime and a microstructure of elementary particles through spin-loop oscillation modes of the spacetime substance itself. The self-replicating quanta following the common logistic equation suggests a pathway for unification between quantum theory, classical physics and thermodynamics.

The QPoD model is still sketchy and much efforts need to be pursued, but our preliminary exploration is encouraging. Many quantum properties emerge naturally, and sometime trivially, from the logistic dynamics of a quantum population that is in a way analogous to what is observed commonly in our environment.

## Acknowledgement

The author acknowledges UQAM for support during sabbatical leave allowing to complete this work. A special thanks to colleagues in various universities who where encouraging in providing support in many discussions, including Serge Robert, Yves Gingras, Louis Vervoort and Louis Marchildon, The author is grateful to the Institut des sciences de l'environnement for very stimulating interdisciplinary milieu where key ideas grew.

## References

[1] Ausloos, M. and M. Dirickx, The Logistic Map and the route to Chaos. From the Beginnings to Modern Applications.

- Understanding Complex Systems. 2006: Springer. ISBN-13 978-3-540-28366-9. 411pp.
- [2] Krapivsky, P.L., et al., A kinetic view of statistical physics. 2010, Cambridge, UK. New York: Cambridge University Press. ISBN 978-0-521-85103-9. 488pp.
- [3] May, R.M., Simple mathematical models with very complicated dynamics. *Nature*, 1976. 261(5560): p. 459-67.
- [4] Couder, Y., et al., Dynamical phenomena: Walking and orbiting droplets. *Nature*, 2005. 437: p. 208.
- [5] Brady, R. and R. Anderson, Why Bounding Droplets are a Pretty good Model of Quantum Mechanics. arXiv:1401.4356v1, 2014.
- [6] Protière, S., A. Boudaoud, and Y. Couder, Particle-wave association on a fluid interface. *Journal of Fluid Mechanics*, 2006. 554(10): p. 85-108.
- [7] Malament, D., The class of continuous timelike curves determines the topology of spacetime. *J. Math. Phys.*, 1977. 18(7): p. 1399-1404.
- [8] Bombelli, L., J. Lee, D. Meyer, R.D. Sorkin, Space-time as a causal set. *Phys Rev Lett*, 1987. 59(5): p. 521-524.
- [9] Sorkin, R.D. and E. Woolgard, A Causal Order for Spacetimes with C0 Lorentzian Metrics: Proof of Compactness of the space of causal curves. *Class. Quant. Grav*, 1996. 13: p. 1971-1994.
- [10] Dowker, F., Causal sets and the deep structure of spacetime. 2005, Imperial Coll., London. p. 17. arXiv:gr-qc/0508109.
- [11] Ambjorn, J., J. Jurkiewicz, and R. Loll, Quantum Gravity, or The Art of Building Spacetime. *Approaches to Quantum Gravity*, 2006. ed D. Oriti, Cambridge University Press. 2006. arXiv: hep-th/0604212v1.
- [12] Ambjorn, J., J. Jurkiewicz, and R. Loll, Emergence of a 4D world from causal quantum gravity. *Phys Rev Lett*, 2004. 93(13): p. 131301. arXiv:hep-th/0404156.
- [13] Ambjorn, J., J. Jurkiewicz, and R. Loll, Causal Dynamical Triangulations and the Quest for Quantum Gravity. *Foundations of Space and Time*, ed J.M. G. Ellis, A Weltman 2010: Cambridge Univ. Press. arXiv: arXiv:1004.0352v1.
- [14] Gurau, R., The 1/N expansion of colored tensor models. *Ann. Henri Poincaré* 2011. 12: p. 829-847. DOI 10.1007/s00023-011-0101-8. arXiv:1011.2726v2.
- [15] Jizba, P., H. Kleinert and F. Scardigli, (2010). Uncertainty relation on a world crystal and it application to micro black holes. *Phys. Rev. D*, D81, 084030. DOI:10.1103/PhysRevD.81.084030. arXiv:0912.2253v2.
- [16] Fermi, E., Un metodo statistice per la determinazione di alcune proprieta dell'atomo *Rend. Acad. Lincei*, 1927. 6(602).
- [17] Thomas, L.H., The calculation of atomic fields. *Proc. Cambridge Philos. Soc.*, 1927. 23: p. 542.
- [18] Keller, J., Unification of Electrodynamics and Gravity from START. *Annales de la Fondation Louis de Broglie* 2002. 37(3): p. 359-410.
- [19] Argaman, N. and G. Makov, Density Functional Theory – an introduction. *American Journal of Physics*, 2000. 69: p. 69-79. DOI:10.1119/1.19375. arXiv:physics/9806013v2.
- [20] Malthus, T.R., An Essay on the Principle of Population. Oxford World's Classics reprint. 1798. 158.
- [21] Verhulst, P.-F., "Notice sur la loi que la population poursuit dans son accroissement. *Correspondance mathématique et physique*, 1838. 10: p.113-121.

- [22] Schlosshauer, M.A., Decoherence and the quantum-to-classical transition. Frontiers collection. 2007, Berlin ; London: Springer. xv, 416.
- [23] Feynman, R., The reason for antiparticles. In R. P. Feynman and S. Weinberg. The 1986 Dirac memorial lectures. 1987: Cambridge University Press.
- [24] Yao, W.-M., Particle Data Group. J. Phys., 2006. G33(1).
- [25] Blanchard, P., Complex analytic dynamics on the Riemann sphere. BAMS, 1984. 11: p. 85-141.
- [26] Lauwerier, H.A., Two-dimensional iterative maps. 1977. In Chaos. Edited by A. V. Holden. :Princeton University Press. Chap 3, p. 58-95. ISBN 0-691-08424-6.
- [27] Lauwerier, H.A., One-dimensional iterative maps. 1977. In Chaos. Edited by A. V. Holden. :Princeton University Press. Chap 3. p. 39-57. ISBN 0-691-08424-6.
- [28] Planck, M., Zur Theorie des Gesetzes der Energieverteilung im Normalspektrum. Verhandlungen der Deutschen Physikalischen Gesellschaft 1900. 2: p. 237.
- [29] Bengtsson, I., and K. Życzkowski, (2006). Geometry of Quantum States. Cambridge. 419pp. Cambridge. ISBN 978-0-521-89140-0.
- [30] Lindblad G., (1976). On the generators of quantum dynamical semigroups, Commun. Math. Phys. 48 119
- [31] Lindblad G., (1983). Non-Equilibrium Entropy and Irreversibility. Delta Reidel. Dordrecht: 1983. ISBN 1-4020-0320-X



**Jean-Pierre Blanchet** received his PhD degree in Physics from the University of Toronto in 1984 and a Master degree in atmospheric physics from McGill University in 1979. His research interests are in the areas of radiative transfer, aerosol particles microphysics, climate modeling, space borne satellite instruments, nonlinear system dynamics and quantum foundation. He has published and co-authored many research articles in reputed international journals including Nature and Science. He has been part of the first IPCC (Nobel Peace Prize 2007). He is currently professor at the Université du Québec à Montréal, director of the ESCER research center, director of the Doctorate program in environmental sciences and lead investigator of the TICFIRE space mission.